JOURNAL OF AGRICULTURAL AND FOOD CHEMISTRY

Acid-Induced Cold Gelation of Globular Proteins: Effects of Protein Aggregate Characteristics and Disulfide Bonding on Rheological Properties

ARNO C. ALTING,*,†,‡,△ MIREILLE WEIJERS,*,†,§,△ ELS H. A. DE HOOG,†,‡ ANNE M. VAN DE PIJPEKAMP,†,∥ MARTIEN A. COHEN STUART,§ ROB J. HAMER,†,§,∥ CORNELIS G. DE KRUIF,†,‡,⊥ AND RONALD W. VISSCHERS†,‡

Wageningen Centre for Food Sciences, Wageningen, The Netherlands, NIZO Food Research, Ede, The Netherlands, Wageningen University and Research Centre, Wageningen, The Netherlands, TNO Nutrition and Food Research, Zeist, The Netherlands, and Van't Hoff Laboratory, Debye Institute, University of Utrecht, Utrecht, The Netherlands

The process of cold gelation of ovalbumin and the properties of the resulting cold-set gels were compared to those of whey protein isolate. Under the chosen heating conditions, most protein was organized in aggregates. For both protein preparations, the aggregates consisted of covalently linked monomers. Both types of protein aggregates had comparable numbers of thiol groups exposed at their surfaces but had clearly different shapes. During acid-induced gelation, the characteristic ordering caused by the repulsive character disappeared and was replaced by a random distribution. This process did not depend on aggregate characteristics and probably applies to any type of protein aggregate. Covalent bonds are the main determinants of the gel hardness. The formation of additional disulfide bonds during gelation depended on the number and accessibility of thiol groups and disulfide bonds in the molecule and was found to clearly differ between the proteins studied. However, upon blocking of the thiol groups, long fibrillar structures of ovalbumin contribute significantly to gel hardness, demonstrating the importance of aggregate shape.

KEYWORDS: Aggregation; cold gelation; whey protein isolate; ovalbumin; thiol-disulfide exchange reaction; fibril formation; ordered structures

INTRODUCTION

The ability to gel is an important function of proteins in food systems. Proteins from different sources can produce gels that vary in textural properties (*1*). Most food protein gels are formed during heating and are therefore referred to as heat-induced gels. For a relatively small number of proteins, gelation at ambient temperature is reported (*2*). One process to achieve this is the so-called cold gelation process. In the first step, a solution of native proteins is heated and soluble aggregates are formed by heating at a pH distant from the isoelectric point and at low ionic strength. Upon cooling, the aggregates remain soluble and no gelation occurs. In the second step, gelation is induced at ambient temperature by reduction of the electrostatic repulsion (*3*), either by adding salt or by changing the pH toward the isoelectric point of the proteins. Gelation caused by lowering the pH is called acid-induced gelation.

* To whom correspondence should be addressed. A.C.A. E-mail: arno.alting@nizo.nl. M.W. E-mail: mireille.weijers@nizo.nl.
† Wageningen Centre for Food Sciences.
‡ NIZO Food Research.
§ Wageningen University and Research Centre.
∥ TNO Nutrition and Food Research.
⊥ University of Utrecht.
△ Both authors contributed equally to the work.

In the literature, several studies have reported cold gelation of whey protein isolate (WPI) (*1*, *3*, *4*−*19*). Most of these concerned the salt-induced type of cold gelation of WPI, and only a few studies dealt with the acid-induced type (*3*, *14*, *15*, *17*−*19*). Previously (*3*, *17*−*19*), we demonstrated that in the acid-induced cold gelation process, first a protein network is formed by physical interactions, which is subsequently stabilized by the formation of disulfide bonds. The formation of disulfide bonds took place despite the acidified conditions and will likely also occur under more favorable conditions in the salt-induced type of cold gelation of WPI. The formation of disulfide bonds was shown to be of great importance for the mechanical properties of cold-set WPI gels and for their physical stability (syneresis) (*3*, *17*−*19*).

Whereas the cold gelation of commercially available WPI was intensively investigated, far less is known about the cold gelation of globular proteins in general. Therefore, in this study, the cold gelation process of ovalbumin was compared with that of WPI. In contrast to WPI or β-lactoglobulin (β-lg), which both form aggregates with a curved strandlike morphology (*18*, *20*), ovalbumin can form soluble fibrillar aggregates (*21*) under the conditions applied in the cold gelation process. β-Lg is the

10.1021/jf034753r CCC: $27.50
Published on Web 01/15/2004

most abundant protein in WPI (>75%) and determines to a large extent the behavior of WPI during heat treatment. Because the different proteins in WPI may have different denaturation kinetics, the use of protein mixtures instead of pure protein fractions may have an impact on the final properties of the gels when heat-set gels are prepared. However, here, cold gelation was used, in which aggregation and gelation take place sequentially, which makes it possible to study the direct relation between aggregate properties and final gel properties. In addition to the shape, other aggregate characteristics, such as size and number of thiol groups, do not differ between aggregates of WPI or β-lg prepared under the same conditions (*3*, *18*, *20*).

Both β-lg and ovalbumin are globular proteins with a net negative charge at neutral pH (isoelectric points around 5). The molecular masses are 18 and 46 kDa for β-lg and ovalbumin, respectively. β-Lg contains two cystines and one cysteine residue, and ovalbumin contains six cysteine residues, two of which form a cystine. For both proteins, the thiol groups are buried in the three-dimensional structure of the native protein but are exposed upon denaturation of the protein molecule. The thiol groups and cystines both play an important role in the heat-induced aggregation of these proteins (*22*, *23*).

In contrast to heat-induced gelation, in which aggregation and gelation occur at the same time, in cold gelation, these two processes occur separately. Here, we took advantage of the fact that in the first step stable soluble aggregates were formed, of which the properties could be controlled before gelation was induced. Covalently linked aggregates of ovalbumin and WPI were prepared, which were comparable in terms of their hydrodynamic diameter, electrophoretic mobility, and number of thiol groups, but were clearly differently shaped. Results on the cold gelation of ovalbumin are discussed and compared to the cold gelation of WPI.

MATERIAL AND METHODS

Reagents and Chemicals. Glucono-δ-lactone (GDL), 5,5′-dithiobis-(2-nitrobenzoic acid) (DTNB), sodium dodecylsulfate (SDS), Rhodamine B, and *N*-ethylmaleimide (NEM) were obtained from Sigma Chemicals (St. Louis, MO). Electrophoresis grade agarose was obtained from Life Technologies (Paisley, Scotland). Phastgel Blue R tablets were from Pharmacia Biotech (Uppsala, Sweden). The WPI BiPro was a kind gift from Davisco Foods International Inc. (Le Sueur, MN). The WPI consisted (based on dry weight) of β-lg (74%), α-lactalbumin (α-lac) (12.5%), bovine serum albumin (5.5%), and immunoglobulins (5.5%). The total amount of proteins in the powder was 97.5%, and it further contained lactose (0.5%) and ash (2%) (*24*). Ovalbumin was purified from fresh chicken egg white based on the procedure of Vachier et al. (*25*). Both protein sources were essentially salt free, and no added salt was used in these experiments.

Preparation of Aggregates. WPI aggregates were prepared at protein concentrations of 3 and 9% (w/w) as described elsewhere (*18*). Ovalbumin was dissolved in double-distilled water at ambient temperature at a protein concentration of 2 and 5% (w/w). Ovalbumin aggregates were prepared by heating the ovalbumin solutions in a water bath for 22 h at 78 °C (*26*).

After they were heated, the dispersions of aggregates were rapidly cooled to ambient temperature in running tap water. The amount of native proteins after the heat treatment was determined with a standard assay involving acid precipitation and gel permeation chromatography (*27*). The dispersions of aggregates were stored at 4 °C until use (typically, within a few days) and diluted to 2% (w/w) with double-distilled water just before the start of the gelation experiments.

Blocking and Determination of Reactive Thiol Groups. The number of accessible thiol groups at the surface of the aggregates before and after chemical blocking was determined using DTNB, also known as Ellman's reagent (*28*) as described elsewhere (*17*). The assay was performed in the absence of urea and SDS, to avoid measurement of nonsurface thiols. NEM was added to a final concentration of 2 mM to block the remaining surface thiol groups (*17*). The effectiveness of this treatment was also checked for ovalbumin by the use of the Ellman's reagens.

SDS-Agarose Electrophoresis. SDS-agarose gel electrophoresis [0.4% (w/w) agarose] was performed as described before (*17*) to determine the differences in molecular size of the differently treated protein aggregates. Aggregates (in solution or gel) were dissolved in an SDS-containing buffer (5% SDS, pH 7.0) to a final protein concentration of 0.5% (w/w). Staining was done with Phastgel Blue R.

Viscosity and Voluminosity. The voluminosity (Φ) of ovalbumin and WPI aggregates in very dilute solutions was determined using Einstein's expression $\eta_r = 1 + 2.5\Phi$ (at a protein concentration of 1g/L). In this expression, η_r stands for the relative viscosity η/η_s, where η is the solution viscosity and η_s is the viscosity of the continuous phase. The concentration-dependent viscosity of dilute solutions of ovalbumin and WPI aggregates (0−6 g/L) (heated at 78 and 68.5 °C, respectively, at different protein concentrations) was measured with an Ubbelohde capillary viscometer placed in a water bath of 20 °C. The voluminosity was determined from the initial slope of the concentration dependence of η_r using Einstein's expression (Φ = slope/2.5).

The intrinsic viscosity was determined using the Huggins equation: $\eta_{sp}/c = [\eta] + k[\eta]^2c$. Extrapolation of the plot of η_{sp}/c vs c to zero protein concentration gives the intrinsic viscosity. In this equation, c stands for the concentration of protein (g/mL). The specific viscosity, η_{sp}, was calculated from $\eta_{sp} = (t - t_0)/t_0$ ($= \eta_r - 1$), where t_0 = the efflux of water and t = the efflux of protein solution in the viscosity measurement using an Ubbelohde capillary viscometer (20 °C). The calculations of both the intrinsic viscosity and the voluminosity were based on at least 10 measurements of the efflux times of the different protein solutions and dilutions.

GDL-Induced Gelation. GDL was added as a powder to the dispersions of aggregates [concentration of protein 2% (w/w)] to induce cold gelation at ambient temperature. To observe gelation of the aggregates around their isoelectric points, it was required to add 0.15 (w/w) and 0.16% (w/w) of GDL to WPI and ovalbumin solutions, respectively. The pH was monitored simultaneously in samples placed in a water bath kept at 25 °C or determined after 21 h of incubation at ambient temperature. The final pH value of both WPI and ovalbumin gels was around 5. The gelation point was determined by means of small deformation measurements (see rheological section).

Turbidity Measurements. Turbidity measurements were made at 25 °C and at a protein concentration of 2% (w/w) on a Cary 1E UV−vis spectrophotometer (Varian) equipped with a temperature controller. The turbidity was measured at 500 nm with time using cuvettes with a path length of 1 mm.

Scattering Techniques. Small angle X-ray scattering (SAXS) measurements were made at the Dutch−Belgian beam-line (DUBBLE) at the European Synchrotron Radiation Facility at Grenoble (France). The energy of the beam was 12.2 (wavelength λ = 1.015 Å) and 8 keV (wavelength λ = 1.55 Å), and the detector was a two-dimensional (512 × 512 pixels) gas-filled detector placed at 8 m distance. The scattering wave vector was between 0.1 and 1.0 nm^{-1} (corresponding to a length scale between 6.3 and 62.8 nm in real space). The temperature of the samples was kept constant at 25 °C.

Small angle neutron scattering was performed as described by Tuinier et al. (*24*). The scattering wave vector was between 0.015 and 0.75 nm^{-1} (corresponding to a length scale between 8.4 and 42.4 nm in real space).

Small angle light scattering (SALS) experiments were done on a custom-built setup (*29*). The scattering wave vector was detected between 0.7 and 3.0 μm^{-1} (corresponding to a length scale between 2 and 9 μm in real space). The protein concentration of the samples was 2% (w/w) in all cases; the temperature was kept at 25 °C. The scattering pattern of the samples was recorded as a function of time during 20 h after the addition of GDL.

Confocal Microscopy. Imaging was performed as described elsewhere (*17*). The protein gels were stained by applying 2 μL of an aqueous solution of 0.05% Rhodamine B. Confocal images were made of the cold-set WPI gels acidified for 24 h. Fast Fourier transform (FFT)

spectra were made from these images, with a range between 0.81 and 160 μm^{-1} (corresponding to a length scale between 39 nm and 7.78 μm in real space).

Rheological Measurements. Small amplitude oscillatory measurements were made with a Carri-Med CLS^2 500 rheometer (TA Instruments, Leatherhead, U.K.) using a sand-blasted (roughened) conical concentric cylinder measuring unit (inner radius, 8.60 mm; outer radius, 9.33 mm). Immediately after the addition of GDL, samples were brought into the concentric cylinder and covered with a thin layer of paraffin oil to prevent evaporation. All experiments were done in oscillation mode at a frequency of 1 $rads^{-1}$ (0.159 Hz) and an applied strain of 1%, which is within the linear region. The formation of a gel network was monitored by the development of the storage modulus (G′) and loss modulus (G″) during 21 h at 25 °C. The initial increase in G′ was defined as the gelation point. The maximum linear strain was determined by a strain sweep experiment. Gel hardness was determined by deformation under a compression force approximately 21 h after the addition of GDL, as described elsewhere (*17*) by means of a texture analyzer (type TA-XT2, Stable Micro Systems Ltd., Godalming, England) equipped with a wire mesh device.

Cryo-Transmission Electron Microscopy (TEM) of Dispersions of Aggregates. Cryo-TEM was done as described elsewhere (*26*), using a Philips CM12 transmission electron microscope operating at 80 kV. Images were recorded digitally by a Gatan 791 CCD camera using the Digital Micrograph software package.

TEM of Acid-Induced Cold-Set Gels. Samples of cold-set gels were fixed in 2.5% glutaraldehyde for 1 h and stored in 0.25% glutaraldehyde at 4 °C for 48 h. The fixed samples were rinsed in distilled water and dehydrated at ambient temperature in a graded series of acetone/water mixtures (70, 80, and 96%) for 15 min each, followed by 100% acetone (2 × 30 min). An epoxy resin, EMBED 812, was infiltrated using graded mixtures of EMBED 812 and acetone in three steps of 1 h each. Final infiltration was done overnight in 100% epoxy resin. The samples were embedded in BEEM capsules and subsequently polymerized at 60 °C for 48 h. After polymerization, thin sections were cut using a Leica Ultracut FCS ultramicrotome and collected on 100 mesh Formvar-coated copper grids. The proteins on the grids were stained for 1 min with Reynold's lead citrate followed by 15 s of saturated uranyl acetate in distilled water. The grids were imaged using a Philips CM12 transmission electron microscope operating at 80 kV of accelerating voltage.

RESULTS AND DISCUSSION

Preparation of Disulfide Cross-Linked Ovalbumin Aggregates. Protein aggregates of ovalbumin were prepared by heating solutions of native proteins at pH 7 and at low ionic strength. For WPI, this resulted in dispersions of protein aggregates consisting of covalently cross-linked protein monomers (*17*, *30*). Agarose gel electrophoresis in the presence of the denaturant SDS was used to demonstrate the formation of aggregates of covalently linked ovalbumin monomers under comparable conditions (**Figure 1**). **Figure 1A** shows that upon prolonged heating of a 3% (w/w) ovalbumin solution at 78 °C, aggregates were formed that did not dissociate in the presence of SDS. Similar to WPI (*17*), the migration velocity of the protein band caused by the ovalbumin aggregates becomes similar to that of the ovalbumin monomers, after addition of DTT (**Figure 1B**). Because DTT is known to disrupt disulfide bonds, the electrophoresis results strongly indicated that like the WPI aggregates, ovalbumin aggregates consisted of disulfide-linked ovalbumin monomers.

The kinetics of denaturation and formation of internally disulfide cross-linked aggregates of ovalbumin were clearly different from that of WPI, where denaturation and formation of disulfide cross-linked aggregates under the applied conditions are reported to go hand in hand (*30*). **Figure 1A** clearly shows that even after heating for 300 min the major part of the denatured ovalbumin has not been converted into aggregates consisting of disulfide cross-linked monomers, whereas after 180 min of heating at 78 °C more than 99% of the native ovalbumin molecules is denatured, insoluble at pH 4.6, and physically aggregated (*31*). Prolonged heating, up to 17 h, was required to form the covalent disulfide bonds in physically aggregated denatured ovalbumin molecules. Kitabatake et al. (*22*) also found that in the early stage of aggregation noncovalent bonding played a major role instead of covalent disulfide bonding. Hence, for denatured ovalbumin, physical aggregation of monomers preceded the formation of internal disulfide bonds within these aggregates. With the aid of SDS-agarose electrophoresis, we determined the time needed at a temperature of 78 °C to form aggregates consisting of covalently cross-linked monomers in which more than 90% of the ovalbumin participated. Independent of the protein concentration, this time was 22 h (**Table 1**).

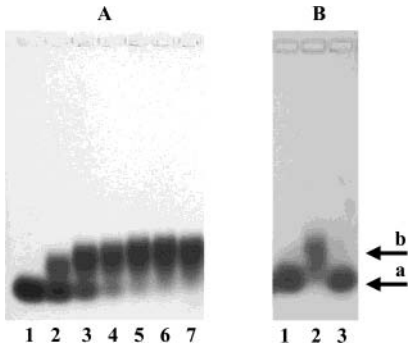

Figure 1. (**A**) SDS agarose gel electrophoresis of heated and unheated ovalbumin solutions (3%, 78 °C). Lane 1, unheated ovalbumin; lanes 2–7, ovalbumin heated for 30, 300, 1026, 2683, and 5000 min and for 8 days. (**B**) SDS agarose gel electrophoresis of ovalbumin aggregates with and without the addition of DTT. Lane 1, unheated ovalbumin (monomers); lane 2, ovalbumin aggregates (5% protein, 22 h, 78 °C) without DTT; and lane 3, ovalbumin aggregates with DTT. Arrow a, protein monomers; arrow b, protein aggregates.

Characterization of Protein Aggregates. *Size.* In the present study, protein solutions were heated at two concentrations, one far below and one close to the reported gelation concentration (*9*, *26*, *32*). As reported elsewhere, the heat treatment of protein solutions at increasing initial protein concentrations resulted in protein aggregates with increasing hydrodynamic radii as determined by dynamic light scattering (DLS) (**Table 1**) (*15*, *18*, *21*, *26*, *27*). For both proteins, the electrophoretic mobility depended on the protein concentration at heating and decreased with increasing protein concentration (not shown). Some caution is justified, because the apparent radii of the aggregates in solution were calculated from a standard cumulant fit of the autocorrelation function of the scattered intensity, assuming that the aggregates have a roughly spherical shape. Hence, these results are only indicative. Indeed, cryo-TEM observations demonstrated that the aggregates prepared did not have a spherical shape (see below).

Shape. Microstructural analysis by means of cryo-TEM showed (**Figure 2**; **Table 1**) that after heat treatment at low ionic strength, a pH around 7, and dependent on the protein concentration, aggregates were formed differing in shape and size, curved strandlike, and long fibrillar aggregates for WPI (*18*, *20*) and ovalbumin (*21*, *26*), respectively. Under the applied conditions, both proteins had a net negative surface charge and formation of soluble linear aggregates is therefore promoted (*33*). Note that the particle sizes as observed by cryo-TEM appeared to be significantly larger than those observed with

Table 1. Characteristics of WPI and Ovalbumin Aggregates

sample[a]	heating conditions	no. of thiol groups (mM)[b]	hydrodynamic radius (nm)[c]	contour length determined by cryo-TEM (nm)	percentage denaturation[d] (%)
3% WPI	24 h, 68.5 °C	0.18	15	20–60	>95
9% WPI	2 h, 68.5 °C	0.34	38	40–100	>95
2% ova	22 h, 78 °C	0.26	12	30–150	>99
5% ova	22 h 78 °C	0.40	35	400–700	>99

[a] The protein concentration given is the concentration at heating (w/w). [b] Determined at pH 7 with Ellman's assay (*28*). The number of thiol groups was determined using $\epsilon_{412nm} = 13\,600\ M^{-1}\ cm^{-1}$ for 2-nitro-5-mercaptobenzoic acid and expressed as the concentration of thiol groups (mM) in a 2% (w/w) dispersion of protein aggregates. Measurements were done in duplicate with an experimental error lower than 10%. [c] The hydrodynamic radii were determined by means of DLS, assuming that the aggregates have a roughly spherical shape (*18*, *26*). [d] According to Alting et al. (*18*) and Weijers et al. (*31*). The concentration of native proteins after the heat treatment was determined with a standard assay involving acid precipitation and gel permeation chromatography (*27*). The concentration of native proteins in the unheated sample was considered as 100% (0% denaturation). Measurements were performed at least in duplicate with an experimental error lower than 5%.

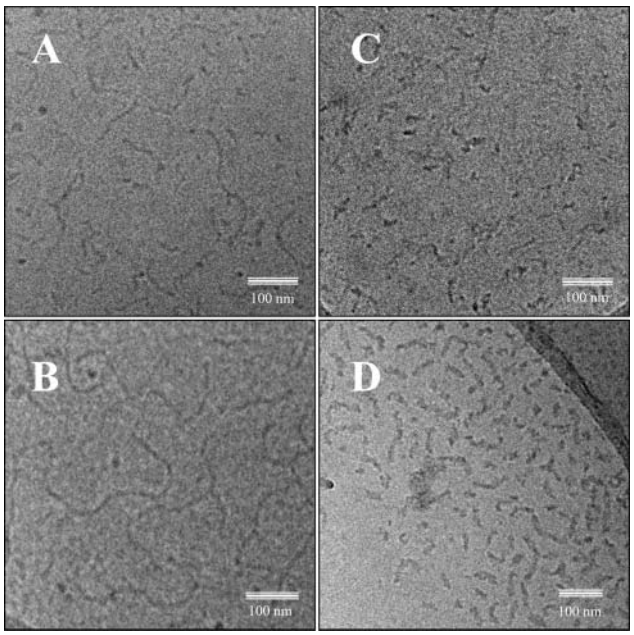

Figure 2. Cry-TEM micrographs of dispersions of aggregates heated at different protein concentrations (w/w). (**A**) 2.5% ovalbumin, 22 h, 78 °C; (**B**) 5% ovalbumin, 22 h, 78 °C; (**C**) 3% WPI, 24 h, 68.5 °C; and (**D**) 9% WPI, 2 h, 68.5 °C.

DLS, which can probably be explained by the elongated shape of the aggregates.

Number of Exposed Thiol Groups. **Table 1** shows that at the point in time that 95−99% of the protein was aggregated into covalently linked monomers, a lower number of thiol groups was detectable for aggregates prepared at a lower initial protein concentration. For WPI, this was explained by differences in the occurrence of oxidation or degradation reactions (*18*, *34*, *35*) caused by a difference in heating time to reach 95% aggregation. The results of ovalbumin heated at different protein concentrations cannot be fully explained in this way, as these were heated for the same period of time. The blocking of the thiol groups by means of a treatment with NEM had no effect on the size as determined with both DLS and agarose electrophoresis for both the WPI and the ovalbumin aggregates.

Acid-Induced Cold Gelation. Before gelation was induced by the addition of GDL, dispersions of aggregates prepared at various protein concentration were diluted to a protein concentration of 2% (w/w). In water, GDL slowly hydrolyzes, yielding gluconic acid, which caused a gradual decrease of the pH and induces gelation of the dispersions of aggregates toward their isoelectric points. The resulting properties of the final cold-set ovalbumin gels such as the appearance and the large deformation mechanical properties clearly differed from cold-set WPI gels.

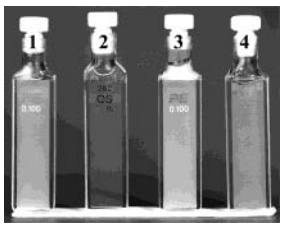

Figure 3. Appearance of cold-set gels [2% (w/w) protein] of ovalbumin and WPI as observed in cuvettes with a path length of 1 mm. (1) WPI, initial protein concentration 9% (w/w); (2) ovalbumin, initial protein concentration 5% (w/w); (3) WPI, initial protein concentration 3% (w/w); and (4) ovalbumin, initial protein concentration 2% (w/w).

Appearance of Cold-Set Gels. The ovalbumin gel prepared from a dispersion heated at a protein concentration of 2% is translucent, and the gel prepared from a dispersion prepared at 5% (w/w) is transparent (**Figure 3**). On the other hand, both of the WPI gels, prepared from dispersions initially heated at protein concentrations of 3 and 9% (w/w), were turbid (see also **Table 2**; A_{500nm} after 21 h). Kitabatake et al. (*22*) also reported the formation of transparent ovalbumin gels using a different gelation method. Visually, treatment with NEM had no influence on the appearance, although small but reproducible differences in turbidity could be determined for WPI (**Table 2**), which is discussed elsewhere (*19*).

Large Deformation Properties. Figure 4 shows the force−distance curves of cold-set gels of both ovalbumin (**Figure 4A**) and WPI (**Figure 4B**) determined by gel penetration measurements. For cold-set gels of ovalbumin, we observed a clear effect of the protein concentration at heating on the gel hardness (**Figure 4A**). More force (approximately six times) had to be applied to penetrate gels prepared from dispersions heated at a protein concentration of 5% (w/w) than gels prepared from dispersions heated at 2% (w/w). Surprisingly, no effect of the thiol-blocking agent on gel hardness was observed. This suggests that instead of the ability to form disulfide bonds, other aggregate characteristics, such as the shape, will contribute to these differences.

As reported previously (*17*, *18*), 2% (w/w) cold-set WPI gels of dispersions initially heated at 9% (w/w) protein were approximately 10 times stronger than gels prepared from dispersions initially heated at 3% (w/w) protein (**Figure 4B**). There, we concluded that the hardness of cold-set WPI gels, in contrast to ovalbumin, is determined by the number of thiol groups rather than by the size of the aggregates or other structural features. **Figure 4B** shows that indeed only a minor

Table 2. Rheological and Scattering Characteristics of Acid-Induced Gelation of Ovalbumin and WPI[a]

sample[b]	G′ (21 h) (Pa)	A_{500nm} (21 h)	initial increase in G′ (gelation point) (min)	initial increase in A_{500nm} (min)	pH at gelation	maximum linear strain (%)
9% WPI	680	0.57	235	200	5.48	55
9% WPI + NEM	663	0.70	240	230	5.57	14
3% WPI	399	0.80	323	263	5.52	11
3% WPI + NEM	435	0.86	300	246	5.59	8
5% ovalbumin	2980	0.045	130	114	5.82	22
5% ovalbumin + NEM	2960	0.044	130	115	5.78	17
2% ovalbumin	1093	0.23	185	169	5.65	11
2% ovalbumin + NEM	1050	0.22	210	195	5.70	11

[a] Values given are average values. Measurements were done at least in duplicate with an experimental error lower than 10% and lower than 5% for WPI and ovalbumin, respectively. [b] The protein concentration given is the concentration at heating. All experiments are carried out at a final protein concentration of 2% (w/w).

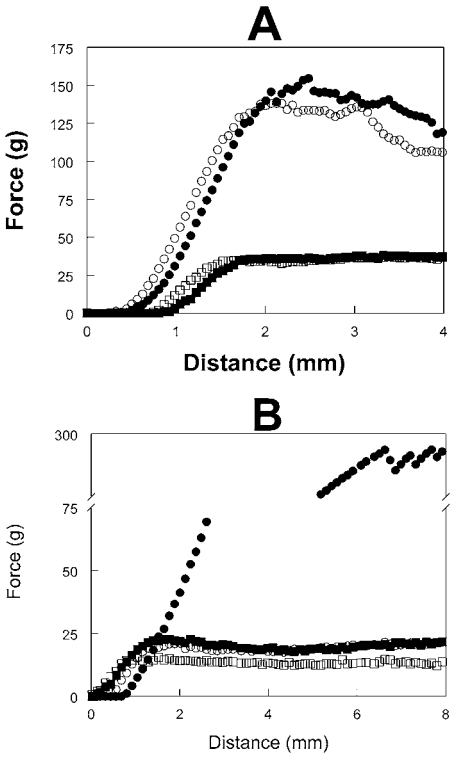

Figure 4. Effect of thiol blocking on the large deformation properties of acid-induced cold-set gels of ovalbumin (**A**) and of WPI (**B**) at a protein concentration of 2% (w/w) after 24 h of acidification. The circles represent the higher initial protein concentrations at heating, 5 (w/w) and 9% (w/w) for ovalbumin and WPI, respectively. The squares represent the low initial protein concentrations at heating, 2 (w/w) and 3% (w/w) for ovalbumin and WPI, respectively. The closed symbols represent the untreated aggregates, and the open symbols represent the NEM-treated aggregates. Note that there is break in the *y*-ordinate in panel **B**.

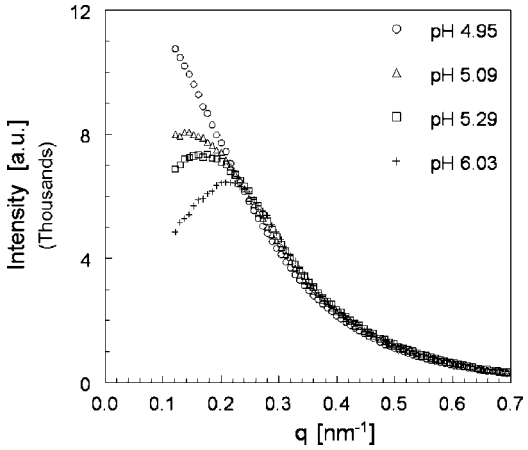

Figure 5. Evolution of the SAXS pattern of a 4% (w/w) solution of ovalbumin aggregates during acidification.

effect of the difference in hydrodynamic diameter (**Table 1**) on the gel hardness remained, if the thiol groups present on the surface of the WPI aggregates were chemically blocked.

To determine the effect of structural properties (size or shape) of protein aggregates on gel hardness, cold-set gels prepared from aggregates treated with a thiol blocker were compared. The effect of the initial protein concentration at heating on gel hardness was much larger for ovalbumin (approximately 600%) than for WPI (approximately 20%). This significant difference cannot be merely explained by differences in the number of elastic effective junctions, which directly relate to the value of G′. The effects of the initial protein concentration on small deformation properties were much smaller (see below). The results can possibly be explained by the formation of entanglements in the case of significantly longer fibrils (40−60 vs 500 nm) in the case of ovalbumin.

Structural Properties. In **Figure 5**, the SAXS patterns are shown for the acid-induced cold gelation of ovalbumin. Before acidification, a clear peak was observed, corresponding to an ordering of aggregates with a typical interparticle distance of approximately 26 nm that shifted toward lower *q*-values upon acidification. Simultaneously, broadening of the peak was observed and finally the peak disappeared, which indicated that the dominant length scale (interparticle distance), present before acidification, disappeared. Comparable results were found on the addition of an increasing amount of sodium chloride (results not shown).

Furthermore, no significant differences between the SAXS patterns of untreated and NEM-treated aggregates were observed during the acidification. For WPI, the same results were obtained but at a significantly higher protein concentration [higher than 6% (w/w)] than for ovalbumin [2% (w/w)], by the use of both SAXS and SANS. At a protein concentration of 9%, typical interparticle distances of approximately 25 and 26 nm were observed for WPI aggregates by the use of SANS and SAXS, respectively.

The SAXS measurements also showed that after a gel is formed at a certain pH (see also **Table 2**), the structure continued to change upon lowering the pH. This suggests that once a gel was formed, structural rearrangements still took place. These observations were confirmed by small deformation and turbidity measurements that continued to increase even after the final pH was reached (see below).

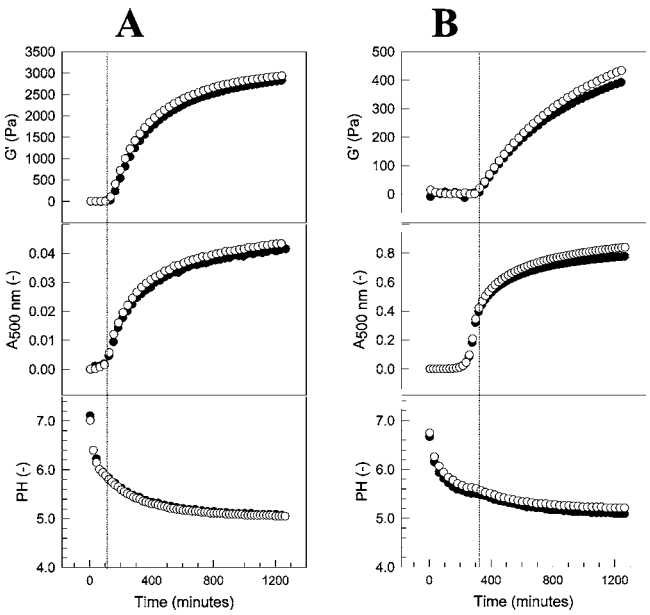

Figure 6. Development of the storage modulus (G′), the turbidity (expressed as A_{500nm}), and the pH with time for ovalbumin, initially heated at 5% (w/w) (**A**), and for WPI, initially heated at 3% (w/w) (**B**), after the addition of GDL. The closed symbols represent the untreated aggregates, and the open symbols represent the NEM-treated aggregates. Note that the *y*-ordinate values are different for panels **A** and **B**.

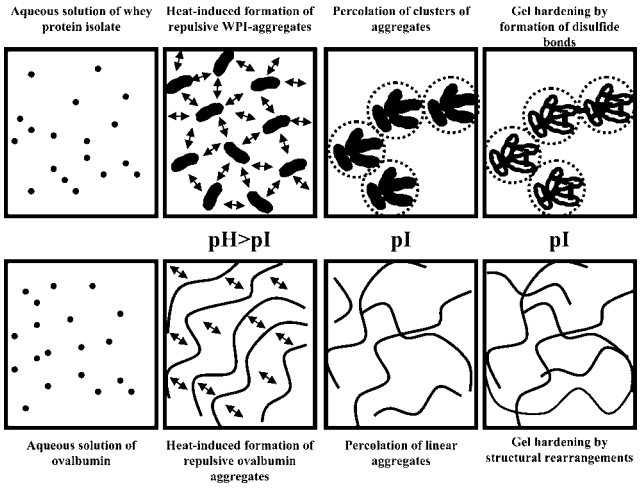

Figure 7. Schematic representation of the acid-induced cold gelation of small (upper panels) and long (lower panels) linear protein aggregates.

Table 3. Intrinsic Viscosity and Voluminosity of Ovalbumin and WPI Aggregates by Heating at Different Protein Concentrations

protein concentration at heating (%)	intrinsic viscosity of the aggregates (mL/g)	voluminosity of the aggregates (mL/g)
WPI 3%	20	7.3
WPI 9%	47.3	21.5
OVA 2%	23.9	10.2
OVA 5.5%	205	80.8

SALS measurements of ovalbumin aggregates in solution showed no dominant length scale. During acid-induced gelation, an increase in scattering intensity, which was not *q*-dependent in the wave vector range measured, was observed, but no dominant length scale was observed. Similar results were obtained for WPI, which were consistent with the confocal microscopy results for WPI described below. The protein structures in the transparent ovalbumin gels could not be visualized probably because these structures were smaller than the resolution of the microscope.

Confocal images were made of the cold-set WPI gels 24 h after GDL addition. No difference was observed in the two-dimesional Fourier spectra of confocal images of gels formed from aggregates with or without thiol blocking treatment. Furthermore, no dominant length scale was observed in this range; therefore, we concluded that both the ovalbumin and the WPI cold-set gels were homogeneous at the length scales probed (over a range of 6.3 nm to 9 μm in real space).

Small Deformation and Scattering Properties. Figure 6 shows representative results of the development with time of the storage modulus (G′), the turbidity (absorbance at 500 nm), and the pH during acidification of dispersions of both ovalbumin (**Figure 6A**) and WPI (**Figure 6B**) aggregates, with and without NEM treatment. In **Table 2**, the results are summarized in six parameters, namely, the G′ after 21 h, the turbidity after 21 h, point in time of the initial increase in G′ (gelation point), point in time of the initial increase in turbidity, the pH at the gelation point, and the maximum linear strain.

Because the acidification curves (pH vs time) of the two proteins were almost identical, results were compared on a time scale instead of a pH scale. There seems to be a relation between the length of the protein aggregates and the point of gelation, defined as the initial increase in G′. Long fibrils [ovalbumin, initially heated at 5% (w/w)] showed the earliest point of gelation in time, and the shortest linear aggregates [WPI, initially heated at 3% (w/w)] showed the latest point of gelation at the same protein concentration. NEM treatment had no significant effect on the gelation point in all cases.

The G′ value reached 21 h after the addition of GDL increases from about 400 Pa for the shortest linear aggregates to approximately 3000 Pa for the longest linear aggregates. G′ and G″ developed concurrently with time, G′ being dominant over the whole time scale measured. Tan δ (G″/G′) was the same (0.13−0.15) for all systems. For gel systems, this value indicates that the viscoelastic gel systems still contained a significant viscous part (G″). NEM treatment of the aggregates had only a minor effect on the development of the storage modulus (G′).

To explain the formation of disulfide bonds and the effect of that on the large deformation properties of acid-induced cold-set WPI gels, we previously (*3*, *17*−*19*) postulated that first a protein network was formed by physical interactions, which was subsequently stabilized by the formation of disulfide bonds. Here, we extended this model (**Figure 7**) and explained the large differences in G′ and turbidity of the various protein systems by differences in overlap concentration. Cold gelation was induced by reduction of electrostatic repulsion between aggregates (*3*). In the case of relatively short linear aggregates (**Figure 7**, upper panels), the aggregates were too small to percolate directly. In this case, the aggregates first became organized in clusters, which were subsequently able to form a space-filling network. This was supported by viscosity measurements (**Table 3**) and by the observation that shorter linear aggregates [WPI 3% (w/w)] showed an increase in turbidity, indicating an increase in aggregate size, before a gel was formed. The number of junctions between the clusters will mainly determine the small deformation properties (in linear region) of the final gels. In the case of relatively long linear aggregates (**Figure 7**, lower panels), formation of a space-filling network occurred immediately after reduction of electrostatic repulsion, resulting in shorter gelation times. In contrast to the short linear WPI aggregates, SAXS measurements showed that the long

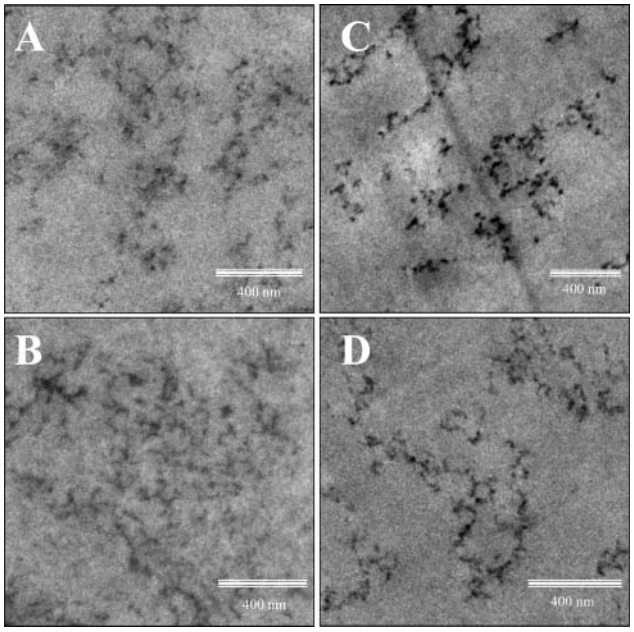

Figure 8. TEM micrographs of 2% (w/w) cold-set protein gels of ovalbumin and WPI initially heated at different protein concentrations (w/w). Ovalbumin, 2% (**A**); ovalbumin, 5% (**B**); WPI, 3% (**C**); and WPI, 9% (**D**).

ovalbumin aggregates maintained a typical interparticle distance at this protein concentration caused by electrostatic repulsion. By the reduction of the repulsion, these aggregates were able to directly form a space-filling network by physical interactions such as hydrophobic interactions and van der Waals attraction. It is known that a protein gel cannot consist of solely entanglements between the structure elements. In addition, no nematic liquid crystalline phases were observed and no disulfide bonds were formed. Therefore, we may conclude that most of the junctions between the individual fibrils will contribute to the small deformation properties, which explain the higher G′ values found for this homogeneous protein gel. The increase of G′ with time, once the final pH is reached, can be explained by the occurrence of structural rearrangements, leading to more junctions. Viscosity measurements on the long fibrillar aggregates (**Table 3**) showed a tremendous increase in intrinsic viscosity and voluminosity of ovalbumin fibrils, initially heated at high ovalbumin concentrations. These results strongly suggest that increased voluminosity (contour length and rigidity) of the fibrillar aggregates leads to shorter gelation times and increased G′.

The maximum linear strain for WPI initially heated at 9% (**Table 2**) was significantly larger than for the other samples. Reduction of the number of thiol groups, either by chemical blocking or by heating at relatively low protein concentration, resulted in a clear reduction of the maximum linear strain. For ovalbumin, the effect of NEM was not significant. However, the maximum linear strain did vary with the size of the ovalbumin aggregates. These results are in good agreement with those obtained from the penetration experiments.

TEM of Acid-Induced Protein Gels. Figure 8 shows TEM micrographs of cold-set gels prepared from protein solutions initially heated at different concentrations. The TEM micrographs confirmed our postulated model (**Figure 7**). WPI gels prepared from an initial protein concentration of 3% (**Figure 8C**) clearly show clusters of small aggregates, and this is less pronounced for WPI gels prepared from an initial protein concentration of 9%, which shows less dense structures (**Figure 8D**). As expected, gels prepared from ovalbumin fibrils show a much more homogeneous structure (**Figure 8B**).The effect of NEM on gel structure was determined for WPI gels and showed no difference with the control. Note that these micrographs were taken from cross-sections through the gel and not from a thin film as in the cryo-TEM measurements; therefore, long fibrillar structures as observed in **Figure 2** cannot be observed.

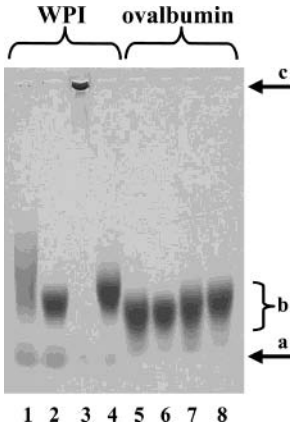

Figure 9. SDS agarose gel electrophoresis of, in SDS-containing buffer, redissolved cold-set gels of untreated and NEM-treated WPI (lanes 1–4) and ovalbumin (lanes 5–8). Lane 1, 3% untreated WPI; lane 2, 3% NEM-treated WPI; lane 3, 9% untreated WPI; lane 4, 9% NEM-treated WPI; lane 5, 2% untreated ovalbumin; lane 6, 2% NEM-treated ovalbumin; lane 7, 5% untreated ovalbumin; and lane 8, 5% NEM-treated ovalbumin. The protein concentrations given are the concentrations at heating (w/w). Arrow a, protein monomers; arrow b, protein aggregates; and arrow c, protein structures that are unable to enter the agarose matrix.

Determination of Disulfide Cross-Linking in Acid-Induced Gels. Finally, to observe differences in the size of the protein structures before and after acid-induced gelation, SDS-agarose electrophoresis was applied (**Figure 9**). The acid-induced ovalbumin gels dissolved more easily in the SDS-containing electrophoresis buffer than the WPI gels. Unexpectedly, but in agreement with the rheological results, electrophoresis of cold-set gels of ovalbumin did not reveal changes in electrophoretic mobility after gelation (**Figure 9**; lanes 5−8). The results of the electrophoretic analysis clearly demonstrated that no disulfide cross-linked structures were formed during the cold gelation of ovalbumin aggregates, although these contained reactive thiol groups.

As reported previously for cold-set gels of WPI (*17*, *18*), disulfide cross-linked protein structures were formed during gelation in the absence of the thiol blocker NEM. The structures had a clearly decreased electrophoretic mobility (increased size) as compared to the electrophoretic mobility of the initial aggregates (before gelation) (**Figure 9**; lanes 1 and 3). The differences in electrophoretic mobility observed between gels prepared from WPI aggregates heated at initial protein concentrations of 3 and 9% were explained by the difference in the number of the thiol groups and therefore in a difference in ability to form disulfide cross-links (*18*). In the presence of NEM, no decrease was observed in electrophoretic mobility (lanes 2 and 4), and the mobility was identical to that before gelation.

Formation of disulfide bonds during the acid-induced gelation is of crucial importance for the properties of cold-set WPI gels (*17*). However, the results of large deformation experiments and the SDS-agarose electrophoresis presented here clearly show that during the acid-induced cold gelation of ovalbumin no additional disulfide bonds were formed, although such bonds did form during the preparation of the ovalbumin aggregates. An explanation might be found in the accessibility of the

disulfide bond in ovalbumin. Different ways for the formation or reduction of disulfide bonds are known, but the one that normally takes place in the aggregation of proteins is the thiol-disulfide exchange reaction (*18*, *36*−*39*). As measured by the use of the Ellman's reagent, the thiol groups of the cysteine residues were accessible for reaction after the heat-induced preparation of ovalbumin aggregates. In contrast, the accessibility of the disulfide bond can be different at conditions during heating (78 °C and pH 7.2) as compared to the conditions during gelation (ambient temperature and pH 5), due to (reversible) conformational changes of the ovalbumin molecule. The decreased accessibility of the disulfide bond will prohibit disulfide cross-linking during gelation. Legowo et al. (*40*) observed that the addition of α-lac, a protein containing four disulfide bonds, significantly increased the hardness of heat-set ovalbumin gels. This also confirms that the thiol group of ovalbumin is available for reaction and that the disulfide bonds in α-lac are accessible for reaction with the heat-exposed thiol groups of ovalbumin, in contrast to the one in ovalbumin. Indeed, Legowa et al. (*40*) demonstrated the contribution of the Cys6-Cys120 disulfide bond of α-lac in the interaction between α-lac and ovalbumin.

Note that WPI is a mixture of proteins. It mainly consists of *β*-lg, but the second major protein is α-lac. Although formation of disulfide bonds was observed in acid-induced cold-set gels of pure *β*-lg (*3*), it was reported that WPI yields stronger gels after induction by high-pressure treatment and that this is also caused by the incorporation of α-lac in the protein network (*41*). The same effect was observed in heat-induced gels of *β*-lg (*42*−*44*).

CONCLUSIONS

For both protein preparations, ovalbumin and WPI, repulsive aggregates were made consisting of disulfide cross-linked monomers. Both type of aggregates possessed exposed thiol groups at their surface (**Figure 7**). At pH 7, the aggregates of both WPI and ovalbumin had a net negative charge and typical interparticle distances in the nanometer range were observed using different scattering techniques. This distance scaled with the protein concentration. If the net charge of the aggregates approached neutrality, the characteristic length scale observed before gelation disappeared, and over a wide range of length scales (nm to *μ*m), no other characteristic length scale could be observed. Cold-set gels were formed by reduction of the electrostatic repulsion (*18*). Therefore, we concluded that during this process the protein system changed from an ordered into a more randomly organized structure. Because formation of the microstructure, as a result of the reduction of electrostatic repulsion, did not depend on aggregate characteristics, it can be defined as a nonprotein specific mechanism; therefore, this mechanism will apply to any type of protein aggregate that is acidified toward its isoelectric point.

Differences in size and shape of the protein aggregates were found to influence small deformation properties of protein gels. Longer aggregates have a lower overlap concentration, which causes gelation to commence earlier and results in more effective junctions, yielding higher G′ values.

Covalent bonds are the main determinants of the gel hardness. The formation of additional disulfide bonds after gelation not only depends on the number of thiol groups but also on the number and accessibility of disulfide bonds in the molecule and may differ significantly from one protein to another. However, in the absence of covalent bonds, long fibrillar structures can also contribute significantly to gel hardness.

ACKNOWLEDGMENT

Marcel Paques and Johan Hazekamp are thanked for their contribution to the (cryo)-TEM measurements, Igor Dolbnya and Wim Bras for their technical assistance at the DUBBLE in Grenoble, Roland Wientjes for his helpful advice concerning the rheological measurements, and Ton van Vliet for fruitful discussions.

LITERATURE CITED

(1) Barbut, S.; Foegeding, E. A. Ca^{2+}-induced gelation of preheated whey protein isolate. *J. Food Sci.* **1993**, *58*, 867−871.
(2) Bryant, C. M.; McClements, D. J. Molecular basis of protein functionality with special consideration of cold-set gels derived from heat-induced whey. *Trends Food Sci. Technol.* **1998**, *9*, 143−151.
(3) Alting, A. C.; de Jongh, H. J. J.; Visschers, R. W.; Simons, J. F. A. Physical and chemical interactions in pH-induced aggregation and gelation of food proteins. *J. Agric. Food Chem.* **2002**, *50*, 4674−4681.
(4) Vreeker, R.; Hoekstra, L. L.; den Boer, D. C.; Agterof, W. G. M. Fractal aggregation of whey proteins. *Food Hydrocolloids* **1992**, *5*, 423−435.
(5) Sato, K.; Nakamura, M.; Nishiya, M.; Kawanari, M.; Nakajima, I. Preparation of a gel of partially heat-denatured whey protein by proteolytic digestion. *Milchwissenschaft* **1995**, *50*, 389−392.
(6) Roff, C. F.; Foegeding, E. A. Dicationic-induced gelation of pre-denatured whey protein isolate. *Food Hydrocolloids* **1996**, *10*, 193−198.
(7) Hongsprabhas, P.; Barbut, S. Ca^{2+}-induced gelation of whey protein isolate: effects of preheating. *Food Res. Int.* **1996**, *29*, 135−139.
(8) Hongsprabhas, P.; Barbut, S. Structure forming processes in Ca^{2+}-induced whey protein isolate cold gelation. *Int. Dairy J.* **1997**, *7*, 827−834.
(9) Hongsprabhas, P.; Barbut, S. Protein and salt effects on Ca^{2+}-induced cold gelation of whey protein isolate. *J. Food Sci.* **1997**, *62*, 382−385.
(10) Hongsprabhas, P.; Barbut, S. Effect of gelation temperature on Ca^{2+}-induced gelation of whey protein isolate. *Lebensm.-Wiss. Technol.* **1997**, *30*, 45−49.
(11) Hongsprabhas, P.; Barbut, S. Effects of N-ethylmaleimide and $CaCl^2$ on cold gelation of whey protein isolate. *Food Res. Int.* **1997**, *30*, 451−455.
(12) Hongsprabhas, P.; Barbut, S.; Marangoni, A. G. The structure of cold-set whey protein isolate gels prepared with Ca^{2+}. *Lebensm.-Wiss. Technol.* **1999**, *32*, 196−202.
(13) Elofsson, C.; Dejmek, P.; Paulsson, M.; Burling, H. Characterization of a cold-gelling whey protein concentrate. *Int. Dairy J.* **1997**, *7*, 601−608.
(14) Ju, Z. Y.; Kilara, A. Gelation of pH-aggregated whey protein isolate solution induced by heat, protease, calcium salt, and acidulant. *J. Agric. Food Chem.* **1998**, *46*, 1830−1835.
(15) Ju, Z. Y.; Kilara, A. Effects of preheating on properties of aggregates and of cold-set gels of whey protein isolate. *J. Agric. Food Chem.* **1998**, *46*, 3604−3608.
(16) Kinekawa, Y.-I.; Foyuki, T.; Kitabatake, N. Effects of salts on the properties of sols and gels prepared from whey protein isolate and process whey protein. *J. Dairy Sci.* **1996**, *81*, 1532−1544.
(17) Alting, A. C.; Hamer, R. J.; de Kruif, C. G.; Visschers, R. W. Formation of disulfide bonds in acid-induced gels of preheated whey protein isolate. *J. Agric. Food Chem.* **2000**, *48*, 5001−5007.
(18) Alting, A. C.; Hamer, R. J.; de Kruif, C. G.; Paques, M.; Visschers, R. W. Hardness of cold set whey protein gels determined by the amount of thiol groups rather than by the size of the aggregates. *Food Hydrocolloids* **2003a**, *17*, 469−479.

(19) Alting, A. C.; Hamer, R. J.; de Kruif, C. G.; Visschers, R. W. Cold-set protein gels; interactions, structure and rheology as a function of protein concentration. *J. Agric. Food Chem.* **2003b**, *51*, 3150−3156.
(20) Le Bon, C. Agrégation et gélification de la β-lactoglobuline: Influence des interactions électrostatiques sur la croissance, la structure et la dynamique des agrégats. These, Université du Maine, France, 2001.
(21) Koseki, T.; Kitabatake, N.; Doi, E. Irreversible thermal denaturation and formation of linear aggregates of ovalbumin. *Food Hydrocolloids* **1989**, *3*, 123−134.
(22) Kitabatake, N.; Hatta, H.; Doi, E. Heat-induced and transparent gel prepared from hen egg ovalbumin in the presence of salt by a two-step heating method. *Agric. Biol. Chem.* **1987**, *51*, 771−778.
(23) Mine, Y.; Noutomi, T.; Haga, N. Thermally induced changes in egg white proteins. *J. Agric. Food Chem.* **1990**, *38*, 2122−2125.
(24) Tuinier, R.; Dhont, J. K. G.; De Kruif, C. G. Depletion-induced phase separation of aggregated whey protein colloids by an exocellular polysaccharide. *Langmuir* **2000**, *16*, 1497−1507.
(25) Vachier, M. C.; Piot, M.; Awedé, A. C. Isolation of hen egg white lysozym, ovotransferrin and ovalbumin, using a quaternary ammonium bound a highly cross-linked agarose matrix. *J. Chromatogr. B* **1995**, *66*, 201−210.
(26) Weijers, M.; Visschers, R. W.; Nicolai, T. Light scattering study of heat-induced aggregation and gelation of ovalbumin. *Macromolecules* **2002**, *35*, 4753−4762.
(27) Hoffmann, M. A. M.; Van Mil, P. J. J. M. Heat-induced aggregation of β-lactoglobulin: role of the free thiol group and disulphide bonds. *J. Agric. Food Chem.* **1997**, *45*, 2942−2948.
(28) Ellman, G. L. Tissue sulfhydryl groups. *Arch. Biochem. Biophys.* **1959**, *82*, 70−77.
(29) De Hoog, E. H. A.; Tromp, R. H. On the phase separation kinetics of an aqueous biopolymer mixture in the presence of gelation: the effect of the quench depth and the effect of the molar mass. *Colloids Surf. A* **2003**, *213*, 221−234.
(30) Roefs, S. P. F. M.; De Kruif, C. G. A model for the denaturation and aggregation of bovine β-lactoglobulin. *Eur. J. Biochem.* **1994**, *226*, 883−889.
(31) Weijers, M.; Barneveld, P. A.; Cohen Stuart, M. A.; Visschers, R. W. heat-induced denaturation and aggregation of ovalbumin at neutral pH described by irreversible first-order kinetics. *Protein Sci.* **2003**, *12*, 2693−2703.
(32) Otte, J.; Ju, Z. Y.; Skriver, A.; Qvist, K. B. Effect of limited proteolysis on the microstructure of heat-induced whey protein gels at varying pH. *J. Dairy Sci.* **1996**, *79*, 782−790.
(33) Doi, E. Gels and gelling of globular proteins. *Trends Food Sci. Technol.* **1993**, *4*, 1−5.
(34) Nashef, A. S.; Osuga, D. T.; Lee, H. S.; Ahmed, A. I.; Whitaker, J. R.; Feeney, R. E. Effects of alkali on proteins. Disulfides and their products. *J. Agric. Food Chem.* **1977**, *25*, 245−251.
(35) Watanabe, K.; Klostermeyer, H. Heat-induced changes in sulfhydryl and disulfide levels of β-lactoglobulin A and formation of polymers. *J. Dairy Res.* **1976**, *43*, 411−418.
(36) Creighton, T. E. Experimental studies of protein folding and unfolding. *Prog. Biophys. Mol. Biol.* **1978**, *33*, 231−297.
(37) Saxena, V. P.; Wetlaufer, D. B. Formation of three-dimensional structure in proteins. Rapid nonenzymatic reactivation of reduced lysozyme. *Biochemistry* **1970**, *9*, 5015−5021.
(38) Shimada, K.; Cheftel, J. C. Sulfhydryl group/disulfide bond interchange reactions during heat-induced gelation of whey protein isolate. *J. Agric. Food Chem.* **1989**, *37*, 161−168.
(39) Monahan, F. J.; German, J. B.; Kinsella, J. E. Effect of pH and temperature on protein unfolding and thiol/disulfide interchange reactions during heat-induced gelation of whey proteins. *J. Agric. Food Chem.* **1995**, *43*, 46−52.
(40) Legowo, A. M.; Imade, T.; Yasuda, Y.; Okazaki, K.; Hayakawa, S. Specific disulfide bond in α-lactalbumin influences heat-induced gelation of α-lactalbumin-ovalbumin-mixed gels. *J. Food Sci.* **1996**, *61*, 281−285.
(41) Ipsen, R.; Olsen, K.; Skibsted, L. H.; Qvist, K. B. Gelation of whey protein induced by high pressure. *Milchwissenschaft* **2002**, *11*/*12*, 650−653.
(42) Rojas, S. A.; Goff, H. D.; Senaratne, V.; Dalgleish, D. G.; Flores, A. Gelation of commercial fractions of β-lactoglobulin and α-lactalbumin. *Int. Dairy J.* **1997**, *7*, 79−85.
(43) Matsudomi, N.; Oshita, T.; Sasaki, E.; Kobayashi, K. Enhanced heat-induced gelation of β-lactoglobulin by α-lactalbumin. *Biosci., Biotechnol., Biochem.* **1992**, *56*, 1697−1700.
(44) Legowo, A. M.; Imade, T.; Hayakawa, S. Heat-induced gelation of the mixtures of α-lactalbumin and β-lactoglobulin in the presence of glutathione. *Food Res. Int.* **1993**, *26*, 103−108.

Received for review July 10, 2003. Revised manuscript received November 21, 2003. Accepted December 8, 2003. The Netherlands organization for the advancement of research (NWO) is acknowledged for providing the possibility and financial support for performing measurements at the DUBBLE.

JF034753R